

# ADVANCED DEEP LEARNING FRAMEWORK FOR LUNG CANCER DETECTION ANALYSIS

<sup>1</sup>Nancy Lydia T <sup>2</sup>Dr. R. Ravi

Department Of Computer Science and Engineering,  
Francis Xavier Engineering College, Tirunelveli –Tamil Nadu, India

## Abstract:

Lung cancer continues to be one of the leading causes of death due to cancer globally, and this underlines the enormous urgency for accurate and early diagnosis techniques. This article presents a newer, deeper analytic framework that uses learning algorithms to improve the detection of lung cancer. The recommended structure capitalizes on a rich dataset containing medical images in order to use convolutional neural network (CNNs) and other deep learning techniques for high precision identification of malignant patterns. Our approach incorporates several pre-processing steps such as image normalization as well as augmentations which enhance robustness and generalization ability of model. The performance metrics utilized during evaluation include accuracy, sensitivity, specificity and AUC-ROC. It is evident from experimental results that there are major improvements over traditional diagnostic methods indicating potentiality with regard to deep learning's role in changing screening and diagnosing processes of lung related cancers. This study adds value in the field of medical imaging analysis by providing a tool that can be used in clinical applications aimed at reducing lung cancer mortality through early diagnosis

**Keywords:** Deep learning; Lung Cancer Detection; Convolutional Neural Networks (CNNs); Medical Image Analysis ; Early Diagnosis

## I. Introduction:

Lung cancer is the most common cancer, With the greatest rates of morbidity and mortality, the primary cause of cancer-related death in the US. In 2018, GLOBOCAN reported approximately 2.09 million new cases and 1.76 million deaths attributable to lung cancer globally [1]. The incidence and mortality rates of lung cancer have been rising significantly worldwide. Among lung cancer cases, approximately 85-88% are classified as non-small cell lung carcinoma (NSCLC), while about 12-15% are categorized as small cell lung cancer (SCLC) . Early diagnosis and intervention are critical to improving the overall 5-year survival rate due to the aggressive nature and heterogeneity of lung cancer.

The detection of lung nodules has been the subject of substantial research over the past 20 years using a variety of medical imaging techniques, such as computed tomography (CT), positron emission tomography (PET), magnetic resonance imaging (MRI), low-dose CT (LDCT), and chest radiograph (CRG) [2]. Although CT is considered the gold standard for lung nodule detection, it can only identify

overt lung cancer and is associated with high false-positive rates and harmful X-ray radiation . LDCT has been proposed as an alternative to reduce radiation exposure while detecting lung cancer . However, mortality remains high among patients undergoing LDCT. The development of 2-deoxy-18F-fluorodeoxyglucose (18F-FDG) PET has improved lung cancer detection performance. This method helps with NSCLC diagnosis by offering semi-quantitative tumour glucose metabolism parameters. Nonetheless, 18F-FDG PET requires further evaluation in NSCLC patients. Emerging imaging techniques like magnetic induction tomography (MIT) are being explored for early-stage cancer detection, although they lack clinical validation in human subjects [3] .

Numerous computer-aided detection (CAD) systems have been extensively studied for lung cancer detection and classification. Compared to trained radiologists, CAD systems offer superior performance in detecting lung nodules and cancers in medical images [4]. Typically, CAD-based lung cancer detection systems comprise four steps: image

processing, region of interest (ROI) extraction, feature selection, and classification. Feature selection and classification are crucial for enhancing the accuracy and sensitivity of CAD systems, relying on image processing to capture reliable features. However, distinguishing between benign and malignant nodules remains challenging. Many researchers have applied deep learning techniques to assist radiologists in making more accurate diagnoses. Studies have confirmed that deep learning-based CAD systems can significantly improve the efficiency and accuracy of medical diagnoses, particularly for lung and breast cancers. These systems automatically extract high-level features from original images using advanced network structures, surpassing traditional CAD systems [5]. Deep learning-based CAD systems still have drawbacks, including high false positive rates, low sensitivity, and time consumption. Thus, a quick, affordable, and extremely sensitive deep learning-based CAD system for lung cancer prediction is desperately needed. Research on deep learning-based lung imaging techniques primarily focuses on pulmonary nodule detection, segmentation, and classification of benign and malignant nodules. Efforts are concentrated on developing new network structures and loss functions to enhance model performance [6,7]. Recent reviews have documented progress in deep learning techniques. However, the rapid development of new methods and applications necessitates continuous updates in the literature.

This research describes current advances in deep learning approaches for lung cancer detection, segmentation, and classification. It includes recent accomplishments, pertinent research difficulties, and future research goals in addition to the most advanced deep learning-based lung cancer detection techniques.

## **2..Literature Survey:**

Lung cancer is a pressing global health concern, with smoking being the primary contributing factor (Banerjee & Das, 2021) [8]. Early detection and accurate diagnosis are crucial for improving patient outcomes, as individuals with lung cancer

have a 10-to 20% probability of surviving five years following diagnosis.(Thanoon et al., 2023)[9] Computational imaging techniques, such as chest X-rays and CT scans, have become common medical procedures for early lung cancer detection.

However, there are still issues with deep learning-based CAD systems, such as high false positive rates, low sensitivity, and time consumption. Therefore, there is an urgent need for a fast, reasonably priced, and highly sensitive deep learning-based CAD system for lung cancer prediction.

The advantages of deep learning for lung cancer detection are manifold. Deep learning models can accurately classify lung nodules based on their location, size, number, consistency, and other factors (Abunajm et al., 2023) [13]. In turn, this can help distinguish between benign and malignant lung tumors and guide appropriate treatment decisions.

However, the adoption of deep learning in clinical practice remains limited due to challenges such as the need for large and diverse training datasets, which can be difficult to obtain in the medical domain.

## **3 .Proposed System:**

The proposed technique employs a combination of rules for type determination. N4ITK is utilized to eliminate noise within the 3D photo and correct bias field. Data segmentation is performed using the region expanding method, while features are extracted using 3D CNN and GLCM algorithms [14]. These extracted features are then passed to the BPNN classifier for further prediction.

The framework is generated to implement the model for discovering and classifying MRI clinical imaging malignancies. Python was chosen for its readability, intuitive data structure, and open-source nature, along with its wealth of graphic packages and included datasets. Therefore, Python programming is preferred over MATLAB for this research[15]. Additional Python libraries such as NumPy, scipy, scikit-learn, TensorFlow, and Keras are employed to construct this recommended model.

The architecture of the recommended model is described below:

a) Datasets

In this model, 3D images in NIFTI format are utilized. The dataset comprises 300 images, each with dimensions of 155240240 pixels. Among these, 150 images are malignant, and 150 are benign. The dataset is divided into two halves, with 70% of the data used for training and 30% for testing. Cancer is discerned from 3D MR input images, categorized by the T1, T2, and Flair (F) modalities, using an advanced learning algorithm [16].

Data sets are collected by Tirunelveli's MEDAL test center. Real-time patient data sets are captured in MAT format, which are then converted to NII format using the MANGO application. NII images are employed in 3D medical imaging for cancer classification.

b) Deep learning framework

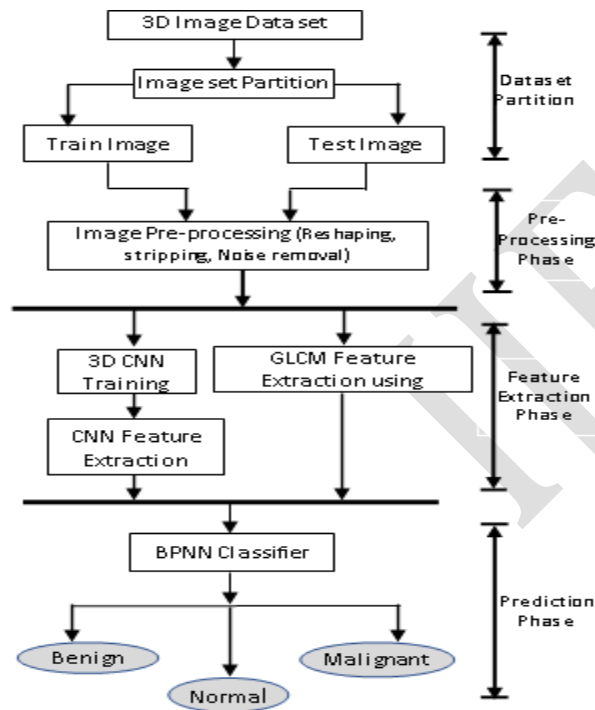


Figure 1 : Deep learning framework

c) Pre-Processing

The images which might be accumulated are pre-processed. The essential techniques inside the Pre-processing level for a flawless input photograph are photograph scaling and noise discount making use of Median filters [17].

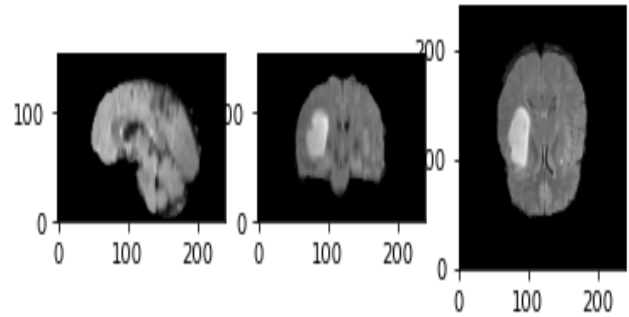


Figure: Input 3d Nii Image

d) Reshaping Images

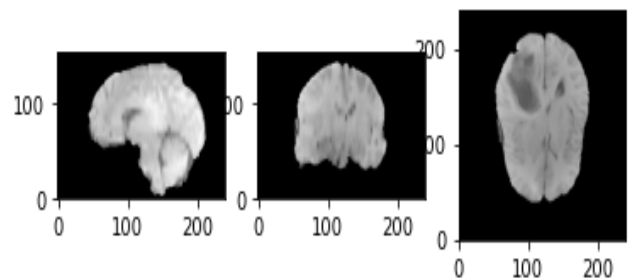
Image resizing is the procedure of scaling images. Reshaping minimizes the number of pixels in a photo, which has some of blessings, inclusive of lowering the time it takes to educate a neural network and simplifying the model [18,19].

To help with photo scaling, OpenCV-Python gives many interpolation techniques.

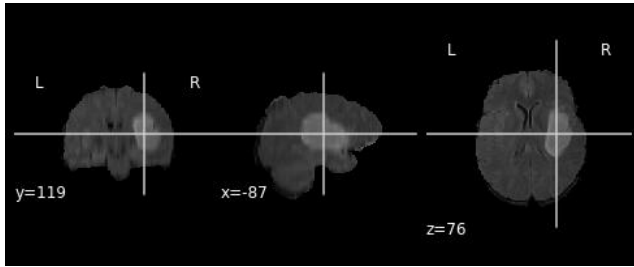
To resize the photo, make use of Scipy and nd photograph, both of which paintings on n-dimensional NumPy arrays. The redesigned matrix is 120\*120\*77 in size.

e) Noise Removal

Noise is described as any degradation within the visual signal caused by an external disturbance. In this research, we evaluate the enter photo and provide findings for median filtering algorithms. Gaussian noise, or the constant noise level in dark regions, accounts for a major quantity of an image's noise. A (typically) small quantity of Gaussian noise is applied to each pixel within the photograph, changing its authentic value [20]. By graphing the degree of distortion of a pixel price towards the frequency with which it happens, a histogram illustrates a everyday distribution of noise.



4.3: Noise Image



4.4: Noise Removal Image

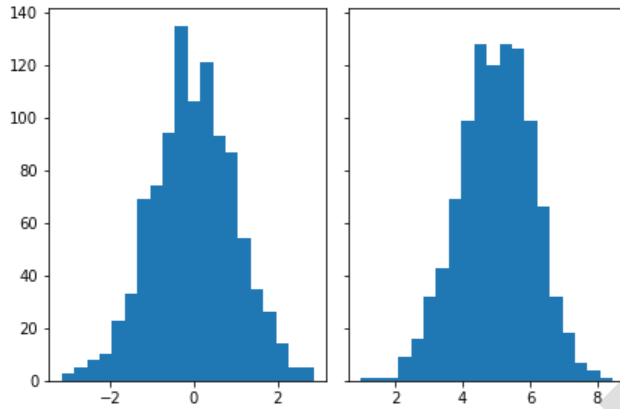


Fig : Histogram of Original and Noise image

Noise = np.random.randn(240, 240, 155)

The median filter's algorithm is as follows:

Step 1: Create a three-dimensional window  $W$  with the dimensions  $3 \times 3 \times 3$ . Assume  $C_x, y, z$  is the pixel to be processed.

Step 2: Find the median of the pixel values in window  $W$  with  $W_{med}$ .

Step 3: Substitute  $W_{med}$  for  $C_x, y, z$ .

Step 4: Repeat steps 1–3 until you've processed all of the pixels in the image.

`median_img = nb.Nifti1Image (average / float(idx + 1), img.affine, img.header)`

#### d) Feature Extraction Using 3D-CNN 3D-CNN Architecture used:

The 3-d-CNN model extract functions are carried out by the convolution + pooling layers. We employ two absolutely-related layers (128 hidden nodes inside the hidden layer), one output layer with four output nodes, and three 3D convolution (Conv) layers to categorise each of the four tasks in our three-D-CNN (8 filters with a kernel size of 7777 inside the first convolution layer, sixteen filters with a kernel size of 5555 within the 2d convolution layer, and 32 filters

with a kernel size of 3333 within the 1/3 Conv layer).

For example, if the input for each 3-d extent was  $240 \times 240 \times 105$ , the output sample at the primary Convolution layer became  $38 \times 64 \times 6 \times 106$  due to a -step stride following the Conv operation, with 8 of them across five filters (i.e., channels); the output pattern at the second Convolution layer became  $17 \times 30 \times 2 \times 320$  due to a two-step stride, with sixteen of them across the 16 channels; the output of the Convolution layer then changed into a 1D vector of 81,674,402 factors and despatched into the fully-linked layer. Training of 3D CNN Model:

These were the settings we used to train our three-D CNN: each node in the Conv and FC layers; rectified linear devices (ReLU) activation features; go-entropy loss characteristic at the output layer; stochastic gradient descent with a minimum studying price of 106 after 20 epochs and a preliminary learning price of 103 (without momentum); the mini-batch length of 32; and dropout with a chance of 0.5 within the output layer. The 3DCNN is also activated by the RELU activation function. The go away-one-challenge-out go-validation method was used to evaluate the overall performance.

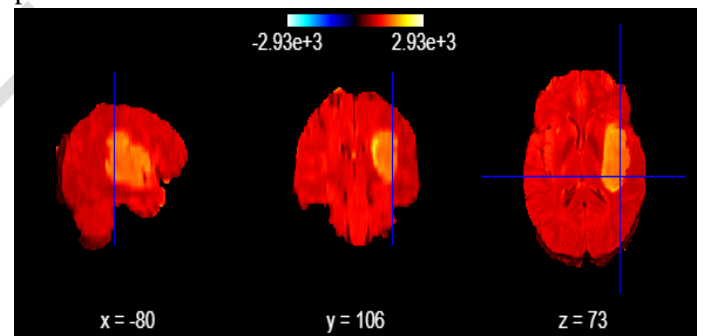


Fig : Segment Image

(In other phrases, 11 people were used to teach the 3-DCNN, and one character was used to test the educated 3-D-CNN, and this technique changed into repeated for each of the 12 take a look at topics). The output of each convolutional layer changed into the input discovered characteristic maps.

#### e) GLCM Feature extraction using PyRadiomics

Radiomics may be employed with most imaging modalities, inclusive of radiography, ultrasonography, CT, MRI, and PET research. When incorporated with clinical, biochemical, and genetic facts, it can increase

the accuracy of diagnosis, diagnosis assessment, and remedy reaction prediction. The maximum discriminatory radiomics characteristic extraction procedures vary depending at the imaging modality and illness being studied, and radiomics research is presently focusing on this.

Characteristics consist of extent, form, surface, density, and depth, in addition to texture, location, and connections with surrounding tissues.

Semantic capabilities are phrases that are frequently used in radiology to designate regions of hobby. Agnostic functions are those that try to constitute lesion heterogeneity the usage of quantitative mathematical descriptors.

For the investigation, the PyRadiomics Python package, model 1.2.Zero, became used to create radiomic traits, the use of recommended default values. It become viable to extract 18 first-order capabilities, 17 shape features, and fifty six texture houses. To generate first-order and texture features, 8 wavelet decompositions were employed (four decompositions for two-dimensional functions), generating a complete of 287 image functions.

| Features    | Values              |
|-------------|---------------------|
| Energy      | 2918821481.0        |
| Entropy     | 4.920992838328338   |
| Kurtosis    | 2.1807729393860265  |
| Mean        | 825.235436306502    |
| Skewness    | 0.27565085908587594 |
| Contrast    | 74.04325876559685   |
| Correlation | 0.39322090748573196 |
| Strength    | 0.9828367173152485  |
| Volume      | 2                   |
| Shape       | 0.5621171627174117  |
| Surface     | 6438.821603779402   |
| Density     | 54.27945170740796   |
| Intensity   | 0.27565085908587594 |
| Texture     | 17.33               |
| Correlation | 0.39322090748573196 |

f) BPNN Classifier

In a multidimensional component space, the practise fashions are class-marked vectors. The strategy's education degree consists only of storing the factor vectors and sophistication names for the guidance assessments. An unlabeled vector (an

inquiry or test point) is sorted through relegating the name that appears the most often a few of the k prepared fashions closest to that question factor. For nonstop factors, Euclidean distance is a extensively used distance metric. In the case of pleasant articulation microarray facts, BPNN has been used in conjunction with affiliation coefficients like as Pearson and Spearman. When the gap metric is determined the usage of professional calculations which includes Enormous Wiggle room Closest Neighbor or Neighborhood parts inquiry, the BPNN characterization accuracy is regularly an awful lot more suitable. In my recommended examine, I use a BPNN Classifier to mix the GLCM and CNN inputs. In my python code, I use the BPNN Classifier from sklearn model preference import train check cut up and sklearn import preprocessing, friends. The GLCM-CNN structure includes a convolution layer (conv3d 1, conv3d 2), sub sampling layers (maxpool1, maxpool2), and a yield layer (thick 5).

The receptive discipline of the extracted 3-d function maps. When the community gets more complex, however, the pooling function can also overlook positive partial function facts, resulting in over- or below-segmentation. We use layer cohesion structure into the 3D-CNN version to get better the spatial information of the 3D characteristic maps. Bilinear interpolation is used to do upsampling. The interpolation of bivariate functions the use of a two-dimensional square grid is known as bilinear interpolation. Post-processing is hired to resolve the issue of misclassified voxels. We take into account cancer with small linked areas to be misclassified voxels with the intention to be disregarded by a threshold method that gets rid of fake most cancers areas with linked regions less than a predetermined threshold. One 10th of the most related vicinity is the adaptively formed preset criterion.

We definitely want to do that to make a prediction. Directly from the output values, the chance of a pattern belonging to every output magnificence can be computed. It might be more nice to convert this output into an exact magnificence prediction. By choosing the class with the finest probability. Another time period for that is the arg max feature.

#### 4. Result And Discussion

The confusion matrices are used to display the tabulation effects of the created CNN below. Non-white rows in confusion matrices are associated with network output training, whereas non-white columns are associated with actual instructions. Diagonally proven are the quantities and possibilities of effectively classified images. The sensitivity is furnished in the closing row, even as the specificity is shown in the ultimate column. Overall accuracy is shown inside the backside-proper field. The better parent represents the range of pics in the non-white containers, whilst the lower range represents the fraction of the entire elegance database within the training or test set. To account for the imbalance of most cancers classes within the database, Tables 5 and 6 provide suggest common accuracy, bear in mind, and F1-score. Following that, it's miles labeled using BPNN and the error-warding off approach is used. This will assist distinguish cancerous cells from healthy ones. Because of the small kernel length, we are able to create a deep community and see greater facts approximately the features. Because the multistage method retains spatial alignment, the model can be examined on any database.

| Images    | Actual | Predicted by proposed Model | Accuracy |
|-----------|--------|-----------------------------|----------|
| Benign    | 156    | 152                         | 0.97     |
| Malignant | 124    | 127                         | 0.98     |
| Normal    | 21     | 24                          | 1.00     |
|           |        | Avg Accuracy                | 0.98     |

**Table 4: Dataset Modeling results**

| Precision | Recall | F1-Score | Accuracy |
|-----------|--------|----------|----------|
| 0.94      | 0.97   | 0.93     | 0.96     |
| 0.97      | 0.85   | 0.92     | 0.96     |
| 0.95      | 0.92   | 0.93     | 0.96     |

**Table 5: BPNN results**

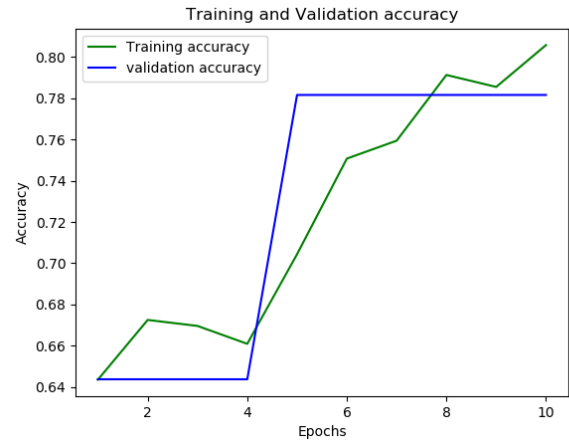


**Fig 5.1: Train and Test Score**

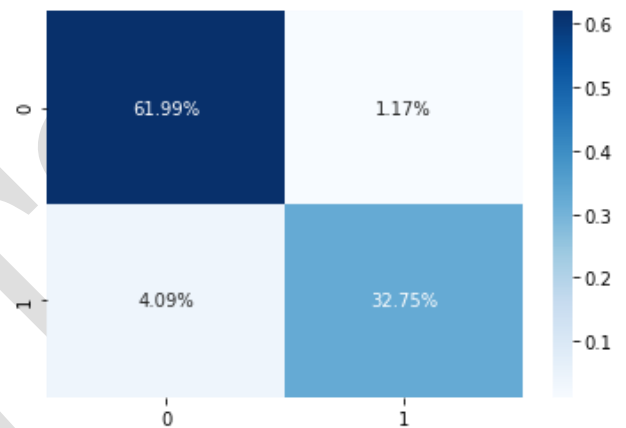


**Figure: Percentage based Confusion Matrix**

#### 5. Conclusion

The BPNN classifier is applied using a modified unique CNN that incorporates GLCM characteristics. When compared to the original CNN, the accuracy of cattle race recognition may be increased by modifying the input layer using the GLCM image. The records records within the input layer has better features than the unique image while using GLCM features, that's a robust point of the amendment. In this method, we do not want to use the segmentation technique for farm animals race class. GLCM traits along with contrast, electricity, and homogeneity have been used. The evaluation and energy snap shots may assist improve the authentic CNN's accuracy, but the homogeneity photograph has a lesser accuracy. Saliency maps provide a excessive degree of precision and may decrease the time it takes to extract GLCM capabilities.

The learning mechanisms utilized by CNN and BPNN

are unique. Combining them might, in most situations, enhance categorisation charges. The combination of BPNN's elevated margin separation and CNN's deep getting to know talents to deal with changes might be the solution to difficult troubles. Although one classifier can be higher than the other in sure cases, fusion might nevertheless provide an appropriate very last class result although one of the classifiers was incorrect due to the nature of the issue.

#### **References :**

1. A novel local mesh color texture pattern for image retrieval system YR Charles, R Ramraj AEU-International Journal of Electronics and Communications 70 (3), 225-233, 2016
2. Local mesh co-occurrence pattern for content based image retrieval CY Rubavathi, R Ravi International Journal of Computer and Information Engineering 9 (6), 1537-1542, 2015.
3. Combined local colour curvelet and mesh pattern for image retrieval system YR Charles International Journal of Business Intelligence and Data Mining 15 (2), 190-203, 2019
4. Opponent Color and Curvelet Transform Based Image Retrieval System Using Genetic Algorithm YR Charles, R Ramraj, 2015
5. Spatially related image mining on very large image collections SN Eymal, CY Rubavathi 2011 International Conference on Emerging Trends in Electrical and Computer.
6. International Journal of Computer and Information Engineering 9 (9), 2112-2119
7. Naik, J.; Prof. Patel, Sagar (2013). Tumor Detection and Classification using Decision Tree in Medical image MRI. IJEDR , ISSN:2321-9939.
8. M. Prastawa, E. Bullitt, and G. Gerig, "Simulation of medical image tumors in MR images for evaluation of segmentation efficacy," Medical Image Analysis, vol. 13, no. 2, pp. 297–311, 2009.
9. A. Ahlgren, R. Wirestam, F. Ståhlberg, and L. Knutsson, "Automatic medical image segmentation using fractional signal modeling of a multiple flip angle, spoiled gradient-recalled echo acquisition," Magnetic Resonance Materials in Physics, Biology and Medicine, vol. 27, no. 6, pp. 551–565, 2014.
10. N. Nabizadeh, N. John, and C. Wright, "Histogram-based gravitational optimization algorithm on single MR modality for automatic medical image lesion detection and segmentation," Expert Systems with Applications, vol. 41, no. 17, pp. 7820–7836, 2014.
11. V. G. Kanas, E. I. Zacharaki, C. Davatzikos, K. N. Sgarbas, and V. Megalooikonomou, "A low cost approach for medical image tumor segmentation based on intensity modeling and 3D Random Walker," Biomedical Signal Processing and Control, vol. 22, pp. 19–30, 2015.
12. Hanh Vu, Hyun-Chul Kim and Jong-Hwan Lee "3D convolutional neural network for feature extraction and classification of fMRI volumes".
13. Guotai Wang, Wenqi Li, S'ebastienOurselin, and Tom Vercauteren "Automatic Medical image Tumor Segmentation using Cascaded Anisotropic Convolutional Neural Networks".
14. M Malathi, P Sinthia "Medical image Cancer Segmentation Using Convolutional Neural Network with Tensor Flow"
15. J. Seetha and S. Selvakumar Raj "Medical image Tumor Classification Using Convolutional Neural Networks"
16. T. Vijayakumar, " Neural Network Analysis for Tumor investigation and Cancer prediction", vol.01, no.02, Journal of electronics and informatics 2019.
17. Pradeep Kumar Mallick, Seuc Ho Ryu, Sandeep Kumar Satapathy, Shruti Mishra, Gia Nhu Nguyen, Prayag Tiwari, "Brain MRI Image Classification for Cancer Detection Using Deep Wavelet Autoencoder-Based Deep Neural Network", IEEE Access, vol 7, 2019.
18. Md Zahangir Alom, Chris Yakopcic, Mst. Shamima Nasrin, Tarek M. Taha & Vijayan K. Asari, "Breast Cancer Classification from Histopathological Images with Inception Recurrent Residual Convolutional Neural Network", Journal of Digital Imaging, 2019.
19. Vijayalakshmi M M, "Melanoma Skin Cancer Detection using Image Processing and Machine Learning", International Journal of trend in scientific Research and Development, vol 3, 2019.
20. Ali Yasar, Ismail Saritas, Heseyin Korkmaz, "Computer-Aided Diagnosis System for Detection of stomach Cancer with Image Processing Techniques", Journal of Medical Ssystems, 2019.



21. Mehwish Bari, Adeel Ahmed, Muhammad Sabir, Sajid Naveed, "Lung cancer detection using digital image processing techniques: A review", *Mehran University Research Journal of Engineering & Technology*, vol 38, 2019.
22. A. Pasumpon Pandian, "Identification and classification of cancer cells using capsule network with pathological images", *Journal of Artificial Intelligence and Capsule Networks*, vol.01, no.01, 2019.
23. Zhang Li, Jiehua Zhang, Tao Tan, Xichao Teng, Xiaoliang Sun, " Deep Learning Methods for Lung Cancer Segmentation in Whole-Slide Histopathology images-- the ACDC@Lung HP Challenge 2019", *IEEE Journal of Biomedical and Health Informatics*, vol 25,2021.
24. Puspanjali Mohapatra, Baldev Panda, Samikshya Swain, "Enhancing Histopathological Breast Cancer Image Classification using Deep Learning", *International Journal of Innovative Technology and Exploring Engineering*", vol 8,2019.
25. AzianAzamimi Abdullah, AafionFonetta Dickson Giong, Nik Adilah Hanin Zahri, "Cervical cancer detection method using an improved cellular neural network (CNN) algorithm", *Indonesian Journal of Electrical Engineering and Computer Science*, vol.14, no. 1, 2019,pp.210-218.
26. Dang N. H. Thanh, V. B. Surya Prasath, Le Minh Hieu, Nguyen Ngoc Hien, "Melanoma Skin Cancer Detection Method based on Adaptive Principal Curvature, Colour Normalisation and Feature Extraction with the ABCD rule", *Journal of Digital Imaging*, vol 33, 2019.
27. Ivan Lorencin, NikolsAndelic, Josip Spanjol, Zlstan Car, "Using multi-layer perceptron with Laplacian edge detector for bladder cancer diagnosis", *Artificial Intelligence in Medicine*, vol 102, 2020.
28. Zhana Fidakar Mohammed, Alan Anwer Abdulla, "Thresholding based White blood cells segmentation from Microscopic Blood Images", *UHD Journal of Science and Technology*, vol 4, no 1, 2020.
29. R. Jothilakshmi, G. Prajwala, "Early lung Cancer detection using machine learning and image processing", *Journal of Engineering Sciences*, vol 11,2020.
30. Yongjun Wang, Baiying Lei, Ahmed Elazab, Ee-Leng Tan, Wel Wang, "Breast Cancer Image Classification via Multi-Network Features and Dual-Network Orthogonal Low-Rank Learning", *IEEE Access*, vol 8, 2020.
31. Mesut Togacar, Burhan Ergan, ZsferComert, "Detection of lung cancer on chest CT images using minimum redundancy maximum relevance feature selection method with convolutional neural networks", *Biocybernetics and Biomedical Engineering*, vol 40, 2020.
32. Muhammad Abduljabbar, Diyar Qader Zeebaree, Adnan Mohsin Abdulazeez, "A Review on Region of interest Segmentation based on Clustering Techniques for breast cancer ultrasound images", *Journal of Applied science and technology trends*, vol. 01, no. 03, 2020.
33. M. Rashidul Hasan, Muntasir AI Kabir, "Lung Cancer detection and classification based on image processing and statistical learning", *Journal of emerging trends in engineering and applied sciences*, vol 11, no 6, 2020.
34. Marc A Bjurlin, Peter R. Carroll, Scott Eggener, Pat F.Fulgham, Daniel J. Margolis, "Update of the standard Operating Procedure on the use of Multiparametric Magnetic Resonance Management of Prostate Cancer", *Journal of urology*, vol 203, 2020.
35. Ada Gjyrezi, Fang Xie, Olga Voznesensky, Prateek Khanna, Carla Catagua, Yang bai, "Taxane resistance in prostate cancer is mediated by decreased drug-target treatment", *the journal of clinical Investigation*, vol 130, no 6, 2020.
36. Wilvertson Tan, Abeer Aisadoon, P. W. C. Prasad, Shahd AI-Janabi, Sami Haddad, Haritha Sallepalli Venkata, "A novel enhanced intensity based automatic registration: Augmented reality for visualization and localization cancer tumors", *The international Journal of /medical Robotics and Computer Assisted Surgery*, vol 16, 2020.
37. Deepa Sheth, Maryellen L.Giger, "Artificial Intelligence in the interpretation of breast cancer on MRI", *Journal of Magnetic resonance Imaging*, vol 51, 2020.
38. Hong Fang, Hongyu Fan, Shan Lin, Zhang Qing, Fatima Rashid Sheykhahmad, "Automatic breast





*cancer detection based on optimized neural network using whale optimization algorithm", International Journal of imaging systems and technology, vol 31, 2021.*

39. Aditya Khamparia, Prakash Kumar Singh, Poonam Rani, Debabrata Samanta, Ashish Khanna, "An internet of health things-driven deep learning framework for detection and classification of skin cancer using transfer learning", *Transactions on Emerging telecommunications technologies, vol 32, 2020.*

40. S.Saravanan, R. Karthigaivel, V. Magudeeswaran, "A brain tumor image segmentation technique in image processing using ICA-LDA algorithm with ARHW model", *Journal of Ambient Intelligence and Humanized Computing, vol 12, 2020.*

41. B. Thiyaneswaran, K. Anguraj, S. Kumarganesh, K. Thangaraj, "Early detection of melanoma images using gray level co-occurrence matrix features and machine learning techniques for effective clinical diagnosis", *International Journal of imaging systems and technology, vol 31, 2021*